Response to Review #1

1. Major Points

1.1. Difference between radar freeboard and scattering horizon height

L22: The statement "altimeters . . . measure sea ice freeboard" is only approximately correct in the case of radar altimeters. The instrument on board CS2 measures a time of flight, which can be related to the height of some radar scattering horizon only where no snow lies in between the scattering horizon and the instrument. When snow is in between and fully penetrated by the radar, the radar range to the scattering surface is overestimated due to slower pulse propagation in the overlying snow. Correcting for this and estimating the height of the ice-snow interface requires knowledge of the overlying snow (Mallett et al., 2020).

This issue surfaces again when the authors identify the radar freeboard as the height from the sea surface to the radar scattering horizon in L28. This is only the case for bare ice. Where overlying snow is present and fully penetrated, the radar freeboard is a finite distance below the ice freeboard (the assumed scattering surface). In the freeboard product used in this manuscript (Kurtz et al., 2014) this displacement is $\underline{h_s}\,(1 - c_s/c)$.

This is relevant to Fig. 1, where h_{rf} *is depicted as being above the ice freeboard. While it may be true that the radar scattering horizon is above the snow-ice interface, in products that assume full radar penetration of the snowpack the radar freeboard is lower than the ice freeboard. Theoretically for total radar penetration and a freeboard depressed to near the water by snow, the radar freeboard can be below the waterline (while the ice freeboard and scattering horizon are above).*

We became aware of that the definition of 'radar freeboard' used in the manuscript is not consistent with the one used in CS2 data-related references (e.g., Kurtz et al., 2014), which is the estimated height of radar scattering horizon before applying the wave propagation speed correction. Therefore, Fig. 1 in the manuscript is replaced by figure AC1-1, by following your suggestion on using different notations for clarity.

Now, the system includes correction terms regarding the wave propagation speed change in the snow layer (F_c), and the displacement of the scattering horizon from the ice surface (F_p) following Kwok and Cunningham (2015) and Armitage and Ridout (2015).

$$F_i = F_r + \left(F_c - F_p\right) \quad \text{(AC1-1)}$$

$$F_c = (\eta_s - 1)\, f h_s \quad \text{(AC1-2)}$$

$$F_p = (1 - f) h_s \quad \text{(AC1-3)}$$

Here, η_s denotes the refractive index of snow layer ($\eta_s = c/c_s$) and f denotes the radar penetration factor, respectively. Combining three equations yields the following relationship.

$$F_i = F_r + (f\eta_s - 1) h_s \quad \text{(AC 1-4)}$$

In the revision, new formulae are introduced for simultaneously solving snow depth and ice thickness even for radar-based freeboard measurements.

1.2 The freeboard product used by the authors has been created with mW99

In the final sentence of the abstract, the authors state:

> *"In conclusion, the developed α-based method has the capacity to derive ice thickness and snow depth, without relying on the snow depth information as input to the buoyancy equation for converting freeboard to ice thickness."*

However, the method presented here works directly from ice freeboard data which can only be derived by relying on snow depth information (Sect. 5.1 & Eq. 15 of Kurtz et al., 2014).

I feel that what the authors would like to present is a way to convert radar freeboards to ice thickness without relying on snow depth data, and this should be done before publication. I think it is possible for the authors to adapt their processing chain to deal with this, although it may complicate things.

Thanks for the suggestion which in fact led to our deeper understanding of radar altimeter remote sensing. Luckily, we were able to include this issue in the retrieval, by modifying Eqs. (5) and (7) of the manuscript (see below for Eqs. (5) and (7) written with new notation), using Eq. (AC1-4).

Eq. (5): $H_i = \left(\frac{\rho_w}{\rho_w-\rho_i}\right) F_i + \left(\frac{\rho_s}{\rho_w-\rho_i}\right) h_s$

Eq. (7): $H_i = \frac{\rho_w}{\rho_w-\rho_i-\alpha\rho_s} F_i$

It is because Eq. (AC1-4) does not include additional unknowns, for given parameterization and assumption on the radar penetration. We assumed $f = 0.84$ for CS2 (Armitage and Ridout, 2015). η_s can be parameterized as a function of the snow density, i.e., $\eta_s=(1+0.51\rho_s)^{1.5}$ (Ulaby et al., 1986). Here we present how the equations were solved.

First, the traditional method for the ice thickness retrieval with the snow depth as input can be written in the following equation by substituting F_i with F_r using Eq. (AC1-4).

$$H_i = \frac{\rho_w}{\rho_w-\rho_i} F_r + \frac{(f\eta_s-1)\rho_w+\rho_s}{\rho_w-\rho_i} h_s \quad \text{(AC1-5)}$$

Then, substituting h_s with αH_i and rearranging the equation yield the equation for H_i as a function of radar freeboard and α, without snow depth information.

$$H_i = \frac{\rho_w}{\rho_w-\rho_i-\alpha\{(f\eta_s-1)\rho_w+\rho_s\}} F_r \quad \text{(AC1-6)}$$

Note that Eq. (AC1-6) becomes equivalent to the equation for the total freeboard if $f = 0$ (no wave penetration into snow layer).

This new setup requires the data processing chain to be modified as well. Here we describe what changes were made (in Sect. 3.3 and 3.4 of the manuscript). First, CS2-like radar freeboard was derived from OIB total freeboard (F_t^{OIB}) and snow depth (h_s^{OIB}). From Eq. (AC1-4) and the relationship $F_i = F_t - h_s$, the radar freeboard can be expressed as follows.

$$F_r^{OIB} = F_t^{OIB} - h_s^{OIB} - (f\eta_s - 1)h_s^{OIB} \quad \text{(AC1-7)}$$

Because the main objective of using OIB data is to evaluate the relative performance of the simultaneous retrieval method when the method is applied to CS2 data, the radar penetration factor (f)

for OIB data processing is also set to be 0.84 (Artimage and Ridout, 2015). In the data processing chain, h_s^{OIB} is removed if it is smaller than the given uncertainty level of the dataset (~5.7 cm) or it is larger than the total freeboard F_t^{OIB}.

The CS2 radar freeboard (F_r^{CS2}) was obtained from CS2 ice freeboard dataset. The CS2 ice freeboard data (F_i^{CS2}) distributed by NSIDC (Kurtz et al. 2017) assume that radar scattering horizon locates at snow–ice interface and applies a wave propagation speed correction. However, the correction was made using the MW99 snow depth (h_s^{MW99}) climatology with an erroneous correction form of $h_c = (1-\eta_s^{-1})\, h_s$, instead of the correct correction form of $h_c = (\eta_s - 1)\, h_s$ (Mallet et al. 2020). Thus, at this point, it is straightforward to derive the CS2 radar freeboard by removing the correction term as in the following equation.

$$F_r^{CS2} = F_i^{CS2} - (1 - \eta_s^{-1}) h_s^{MW99} \quad \text{(AC1-8)}$$

Finally, analyses in the first version of the manuscript are conducted again using the radar freeboard rather than using the ice freeboard. This time SIC criteria for α calculation was set to be 95% (original: 98%) for a wider coverage. Figs. AC1-2 to AC1-5 are the reprocessed results which will replace the figures in the manuscript. Despite of these changes, we find little changes in the conclusions we made in the first version of the manuscript. In addition, for more comprehensive information, snow depth comparison results are provided in Fig. AC1-5.

1.3 Uncertainty Analysis

The authors state in their Discussion and Conclusions section:

> *Overall, the developed α-based method yields ice thickness and snow depth, without relying on a priori 'uncertain' snow depth information, which results in uncertainty in the ice thickness retrieval.*

They are of course correct to identify that uncertainty in snow depth leads to uncertainty in the ice thickness retrieval. To avoid having to quantify snow depth, they instead rely on a parameter equal to h/H, which they empirically derive from the temperature of the air-snow and ice-snow interfaces.

Clearly there is significant uncertainty in the value of α, and the authors should try to quantify how this propagates through into uncertainty in ice thickness. It's possible that their α parameter is more uncertain than other published data for h, and if so this method will deliver lower quality estimates of H than the traditional method.

It seems (looking at Fig. 1 of this review) that a given error in α would have a more serious impact on H than the same error in h, because the gradients of the lines are much more similar in on the left panel of Fig. 1 than on the right. This issue scales with the alpha parameter (i.e. as the freeboard goes down), and at high α very small uncertainties in alpha will lead to large uncertainties in H.

As alpha becomes so large that the freeboard tends to zero (not that uncommon in the Atlantic sector of the Arctic), the method seems to lose its usefulness, whereas the traditional method continues to function. That is to say in the case of near-zero freeboard, the traditional method still provides an

estimate of H, but that proposed by the authors does not (see Eq. 7 as $h_f \rightarrow 0$).

This is addressed in L161/162, where a critical value is given for alpha, and it is explained that for alpha above this value data are not produced. How often does this occur? And what is the effect on H of small errors in alpha just below this critical threshold?

To identify the uncertainty of simultaneous method, snow depth error (Δh_s) equivalent to α error ($\Delta\alpha$) is calculated for chosen three representative sea ice conditions (thicker / moderate / thinner). The Simultaneous method showed a small sensitivity to $\Delta\alpha = 0.03$, which is RMSE value of the regression equation. On the other hand, sensitivity was greater when radar freeboard was used, especially for thinner ice where α is close to α_{crit}. In case of ice thickness error (ΔH_i), gap of sensitivity between total freeboard and radar freeboard methods was reduced because ΔH_i is more sensitive to Δh_s when the total freeboard is used. This characteristic of sensitivity is consistent with results from OIB analysis.

Majority of data used in this study belong to moderate or thicker ice and retrieved α rarely exceeds α_{crit}. Therefore, there should not be many cases having great uncertainty that might be expected from thinner ice condition. As a matter of fact, it seems that retrieved α shows reasonable values upon presumed thermodynamic condition. Areas where thermodynamic condition is not met are located at around the marginal ice zones and in the east of Greenland.

Details can be found in Appendix B (will be included in the revised manuscript). In addition, we clarify that "a priori 'uncertain' snow depth in formation' is MW99 snow depth climatology.

2. Minor Points

2.1. General

• L21: The authors should consider directing the reader to Laxon et al. (2003) when illustrating that thickness has been estimated for nearly two decades.

Laxon et al. (2003) is now included in the manuscript.

• When discussing studies indicating the height difference between the scattering horizon and the snow-ice interface, the authors should consider directing the reader to Nandan et al. (2017) and Willatt et al. (2010, 2011).

Nandan et al. (2017) and Willatt et al. (2011) are now referred in the manuscript. Because characteristic of sea ice is different between Arctic and Antarctic, study on Antarctic sea ice by Willatt et al. (2010) is not included.

• L62 & 64: Define RTM before using the acronym

The acronym 'RTM' stands for 'Radiative Transfer Model'. It is now defined in the manuscript.

• The font sizes of some annotations to Figure 3 should be increased so as to be legible and comparable to the (a), (b), (c) lettering.

Annotation is now increased to be legible (see Fig. AC1-6).

• In Fig. 2, the box that reads 'Find temperature discontinuity point'. It is my understanding that the temperature is continuous (but not a smooth function), and therefore it has no discontinuities (but its gradient does). Should this box then read 'Find temperature gradient discontinuity point'?

Yes, what discontinuous is temperature gradient, not temperature. The text now reads 'Find temperature gradient discontinuity point' (see Fig. AC1-7).

• I think the notation of H and h in combination with h_f, h_{rf} and h_{tf} is confusing to the casual reader. For instance, the fact that h and h_f look so similar but are in fact unrelated confused me initially. Even changing $H \rightarrow H_{ice}$ and $h \rightarrow h_{snow}$ would clarify this.

Following your comment, we have changed our notations (see Sect 1.1 in this response).

2.2. Validation of H against OIB Data

The authors are able to create two products from freeboard data obtained by OIB and CryoSat-2, one for snow depth (h), and one for ice thickness (H). They then rightly try to assess the quality of these data products against other datasets, namely the OIB snow depth and ice thickness data. There are at least five algorithms published to process the raw OIB radar returns into along-track snow depth data, and they produce a spread in the mean snow depth (Kwok et al., 2017). 'Validation' of a model or data implies comparison to true or certain values, and it is unclear which OIB snow depth product (if any) represents the truth. This limits the strength of the validation exercise. Nonetheless, I understand that OIB snow depth values have historically been taken as the truth in published work so this is a perhaps not a big issue. It might also be argued that the spread of different OIB data is sufficiently small relative to other methods of snow depth estimation to allow OIB to approximate the truth for validation purposes.

I feel that there is however a more significant issue with the authors' claims to have 'validated' their ice thickness data against OIB ice thickness data (H_{OIB}). OIB aircraft instruments do not measure thickness (H_{true}) directly, but instead estimate it based on freeboard, snow depth, snow density and ice density values. As such, OIB thickness data (while likely to be the most accurate data on H_{true} outside of in-situ measurement), undoubtedly suffer from biases involving snow depth, snow density and ice density, and therefore should not be mistaken for H_{true}.

The technique for determining H_{OIB} is very similar to that presented in this manuscript: the authors use identical freeboard, snow density and ice density values to estimate thickness with the hydrostatic equilibrium assumption. Given these similarities, comparing the thickness estimates in this paper with OIB thickness estimates doesn't really qualify as independent validation.

It seems more like the exercise of comparing H estimates is in fact comparing the novel snow depth estimates with OIB snow depths (Fig 7 top row; a valuable analysis), and then investigating how that singular difference propagates into sea ice thickness estimates. I suspect that the strong agreement between the two datasets presented in the middle row of Fig. 7. is largely a result of the identical radar freeboards and geophysical parameters used in each processing chain.

After all, much of sea ice thickness is determined by radar freeboard information, independent of snow data. The fact that the 'simultaneous' method matches H_{OIB} data more closely than MW99 is therefore evidence that the snow depth product produced by the 'simultaneous' method is closer to OIB snow depths than MW99 (because everything else is equal).

I think it is perfectly reasonable (and in fact expected) to compare H estimates from the new method with H_{OIB}. However, I think this should be presented as a 'comparison with' or 'evaluation against' OIB data, rather that implying that the new data are being validated against some true value. It is also an understandable bit of reasoning to say that values which are closer to H_{OIB} are likely to be closer to H_{true}, but if this assumption is made it should be stated explicitly.

We agree upon your notion that snow depth and ice thickness comparisons are the same problem. To address your comment, we first clarified how H_i^{OIB} is calculated in Sect 3.3. Then, we changed the subtitle of Sect 4.2 from '*Validation* against OIB estimates' to '*Evaluation* against OIB estimates'. Finally, *validation* on ice thickness contents were modified in the direction to address that the estimated snow depth showing a more consistency with h_s^{OIB} implies improved ice thickness. Accordingly, the snow depth comparisons between $h_s(\alpha^{sat}, F_r^{OIB})$ vs. h_s^{MW99} and $h_s(\alpha^{sat}, F_r^{CS2})$ vs. h_s^{MW99} are included in Fig. AC1-5.

2.3. Limitations of Other Data

L66 - 69: Other approaches worth mentioning are snow depth retrieval using dual-frequency altimetry (Guerreiro et al., 2016; Lawrence et al., 2018, Kwok and Markus, 2018), snow on sea ice model accumulating snowfall from reanalysis (Petty et al., 2018), multilinear regression (Kilic et al., 2019), and the neural network approach (Braakmann-Folgmann and Donlon, 2019). However, these methods do not satisfactorily meet the criteria required for freeboard to ice conversion over the entire Arctic Ocean basin scale or multi-year time scale.

The approach of Guerreiro et al. (2016) and Lawrence et al. (2018) are limited latitudinally by the AltiKa orbital inclination and Lawrence et al. (2018) additionally through calibration with OIB which only operates in Spring. As the authors identify, they are limited in spatial or temporal extent. While there are limitations to the data products of Petty et al. (2018), Kilic et al. (2019) and Braakmann-Folgmann and Donlon (2019), it's not obvious that these can be characterized by failure to cover the entire basin on a multiyear timescale. As such, the statement on L69 that they do not satisfactorily meet these criteria should be clarified.

The purpose of this paragraph was to introduce recent researches to readers. Therefore, the last sentence describing limitations of other data, which is not necessary, is removed. In case of Petty et al. (2018), we decided to not include it in the text to keep manuscript's focus on remote sensing, as characteristic of their product seems to be closer to model than remote sensing. Accordingly, paragraph

will be modified as:

"Other *satellite remote sensing* approaches worth mentioning are snow depth retrieval using dual-frequency altimetry (Guerreiro et al., 2016; Lawrence et al., 2018, Kwok and Markus, 2018), multilinear regression (Kilic et al., 2019), and the neural network approach (Braakmann-Folgmann and Donlon, 2019)."

2.4. Rainbow Color Schemes

Where possible, authors should avoid presenting continuous data with 'rainbow' color schemes as in Figures 6 & 8. This is because (among other reasons) the scheme tends to imply sharp transitions in the data where they do not exist (Borland and Taylor, 2007). Alternatives for geoscientists are given by Light and Bartlein (2004), Stauffer et al. (2015) and Thyng et al. (2016).

Thanks for valuable comment. We changed our color scheme to generate figures from 'jet' from 'viridis', which is perceptually uniform colormap, available in matplotlib/python. Figs. AC1-2 and AC1-4 are new plots with the new color scheme.

References

Armitage, T. W. K., and Ridout, A. L.: Arctic sea ice freeboard from AltiKa and comparison with CryoSat-2 and Operation IceBridge, Geophys. Res. Lett., 42, 6724–6731, doi: 10.1002/2015GL064823, 2015.

Braakmann-Folgmann, A., and Donlon, C.: Estimating snow depth on Arctic sea ice using satellite microwave radiometry and a neural network, Cryosphere, 13, 2421–2438, doi: 10.5194/tc-13-2421-2019, 2019.

Guerreiro, K., Fleury, S., Zakharova, E., Rémy, F., and Kouraev, A.: Potential for estimation of snow depth on Arctic sea ice from CryoSat-2 and SARAL/AltiKa missions, Remote Sens. Environ., 186, 339–349, doi: 10.1016/j.rse.2016.07.013, 2016.

Kilic, L., Tonboe, R. T., Prigent, C., and Heygster, G.: Estimating the snow depth, the snow-ice interface temperature, and the effective temperature of Arctic sea ice using Advanced Microwave Scanning Radiometer 2 and ice mass balance buoy data, Cryosphere, 13, 1283–1296, doi: 10.5194/tc-13-1283-2019, 2019.

Kurtz, N. T., Galin, N., and Studinger, M.: An improved CryoSat-2 sea ice freeboard retrieval algorithm through the use of waveform fitting, Cryosphere, 8, 1217–1237, doi: 10.5194/tc-8-1217-2014, 2014.

Kurtz, N. and Harbeck, J.: CryoSat-2 Level-4 Sea Ice Elevation, Freeboard, and Thickness, Version 1, National Snow and Ice Data Center, doi: 10.5067/96JO0KIFDAS8, 2017.

Kwok, R., and Cunningham, G. F.: Variability of Arctic sea ice thickness and volume from CryoSat-2, Phil. Trans. R. Soc. A, 373(2045), 20140157, doi: 10.1098/rsta.2014.0157, 2015.

Kwok, R., and Markus, T.: Potential basin-scale estimates of Arctic snow depth with sea ice freeboards from CryoSat-2 and ICESat-2: An exploratory analysis, Adv. Space Res., 62(6), 1243–1250, doi: 10.1016/j.asr.2017.09.007, 2018.

Lawrence, I. R., Tsamados, M. C., Stroeve, J. C., Armitage, T. W. K., and Ridout, A. L.: Estimating snow depth over Arctic sea ice from calibrated dual-frequency radar freeboards, Cryosphere, 12, 3551–3564, doi:10.5194/tc-12-3551-2018, 2018.

Laxon, S., Peacock, N., and Smith, D.: High interannual variablility of sea ice thickness in the Arctic region, Nature, 425, 947–950, doi: 10.1038/nature02050, 2003.

Mallett, R. D. C., Lawrence, I. R., Stroeve, J. C., Landy, J. C., and Tsamados, M.: Brief communication: Conventional assumptions involving the speed of radar waves in snow introduce systematic underestimates to sea ice thickness and seasonal growth rate estimates, The Cryosphere, 14, 251-260, doi: 10.5194/tc-14-251-2020, 2020.

Nandan, V., Geldsetzer, T., Yackel, J., Mahmud, M., Scharien, R., Howell, S., King, J., Ricker, R., and Else, B.: Effect of Snow Salinity on CryoSat-2 Arctic First-Year Sea Ice Freeboard Measurements, Geophys. Res. Lett., 44(20), 10,419–10,426, doi:10.1002/2017GL074506, 2017.

Petty, A. A., Webster, M., Boisvert, L., and Markus, T.: The NASA Eulerian Snow On Sea Ice Model (NESOSIM) v1.0: initial model development and analysis, Geosci. Model Dev., 11(11), 4577–4602, doi: 10.5194/gmd-11-4577-2018, 2018.

Ulaby, F. T., Moore, R. K., and Fung, A. K.: Microwave remotesensing: Active and passive, Volume 3-From theory to applications, 1986.

Willatt, R. C., Giles, K. A., Laxon, S. W., Stone-Drake, L., and Worby, A. P.: Field inves-tigations of Ku-band radar penetration into snow cover on antarctic sea ice, IEEE Transactions on Geoscience and Remote Sensing, 48, 365-372, doi: 10.1109/TGRS.2009.2028237, 2010.

Willatt, R., Laxon, S., Giles, K., Cullen, R., Haas, C., and Helm, V.: Ku-band radar penetration into snow cover on Arctic sea ice using airborne data, Annals of Glaciology, 52, 197–205, doi: 10.3189/172756411795931589, 2011.

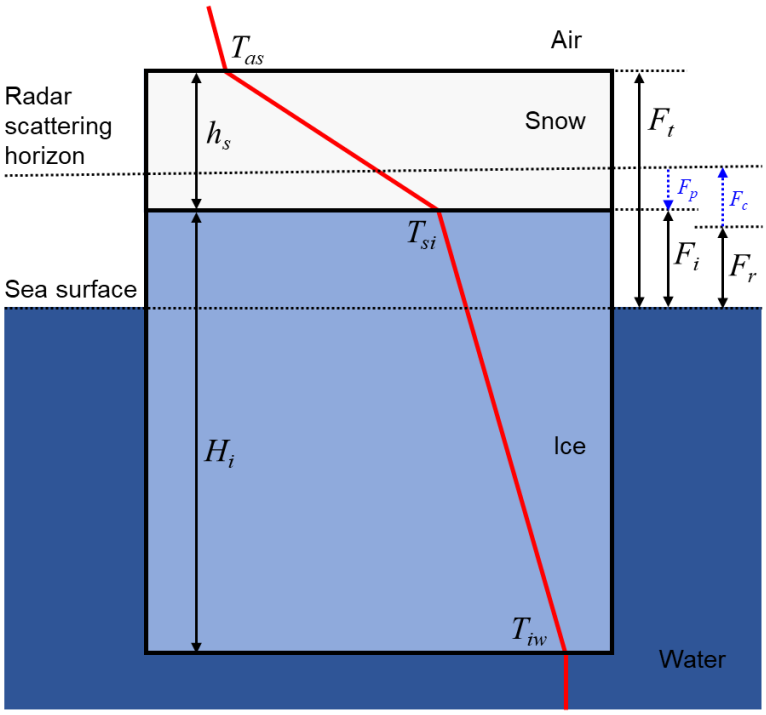

Figure AC1-1. Schematic diagram of a typical snow–ice system during the winter. Snow depth (h_s), ice thickness (H_i), total freeboard (F_t), radar freeboard (F_r), and ice freeboard (F_i) are indicated. Correction terms regarding the wave propagation speed change in snow layer (F_c) and the displacement of the scattering horizon from the ice surface (F_p) are indicated by blue arrows. Red line denotes a typical temperature profile with air–snow interface temperature (T_{as}), snow–ice interface temperature (T_{si}) and ice–water interface temperature (T_{iw}). *In the text, change was also made on the notation for the bulk densities of materials (ρ_i: density of sea ice, ρ_s: density of snow, ρ_w: density of sea water).*

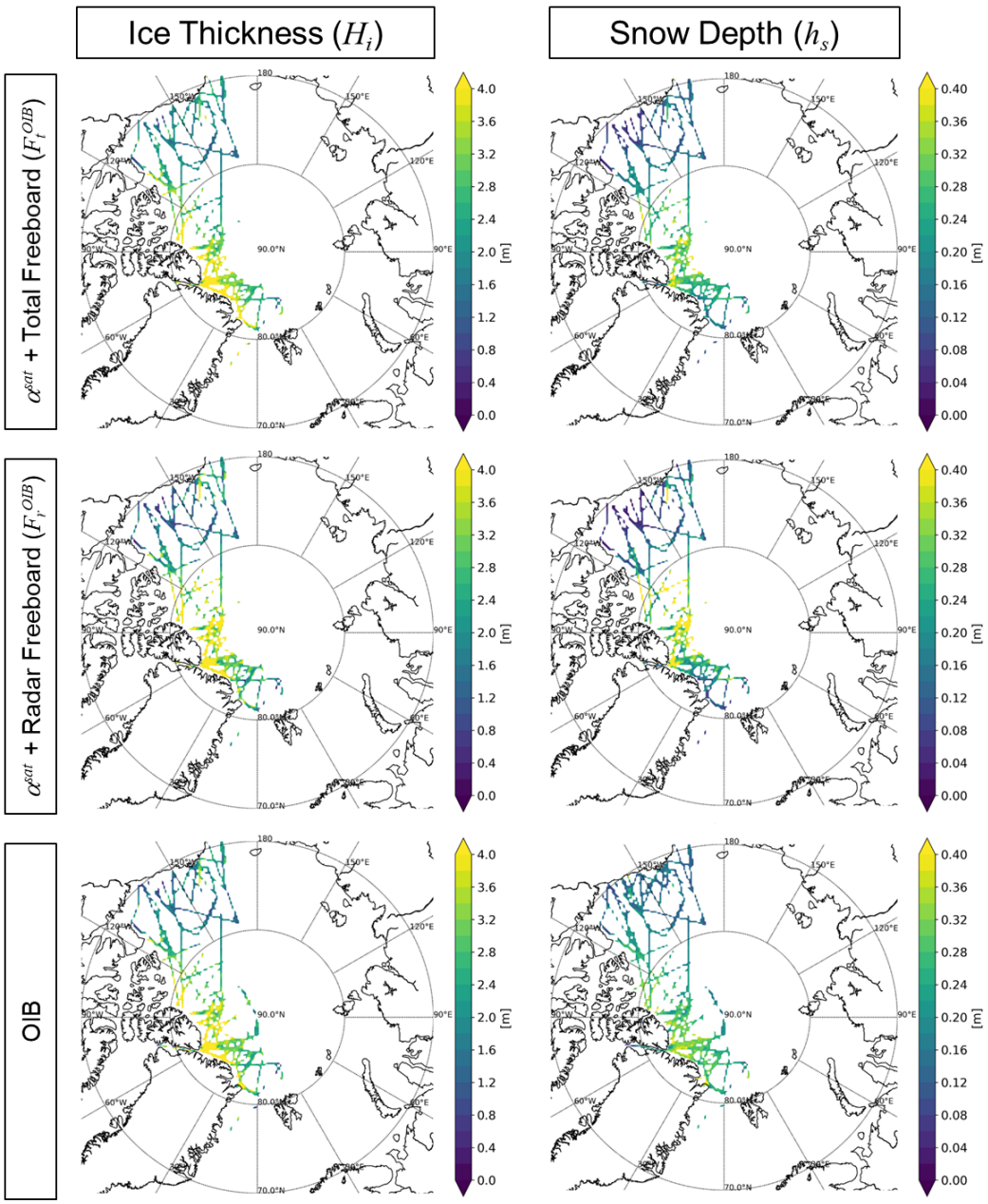

Figure AC1-2. Simultaneously retrieved ice thickness and snow depth from OIB total/radar freeboard in March of the 2011–2015 period. Corresponding OIB products are at the bottom.

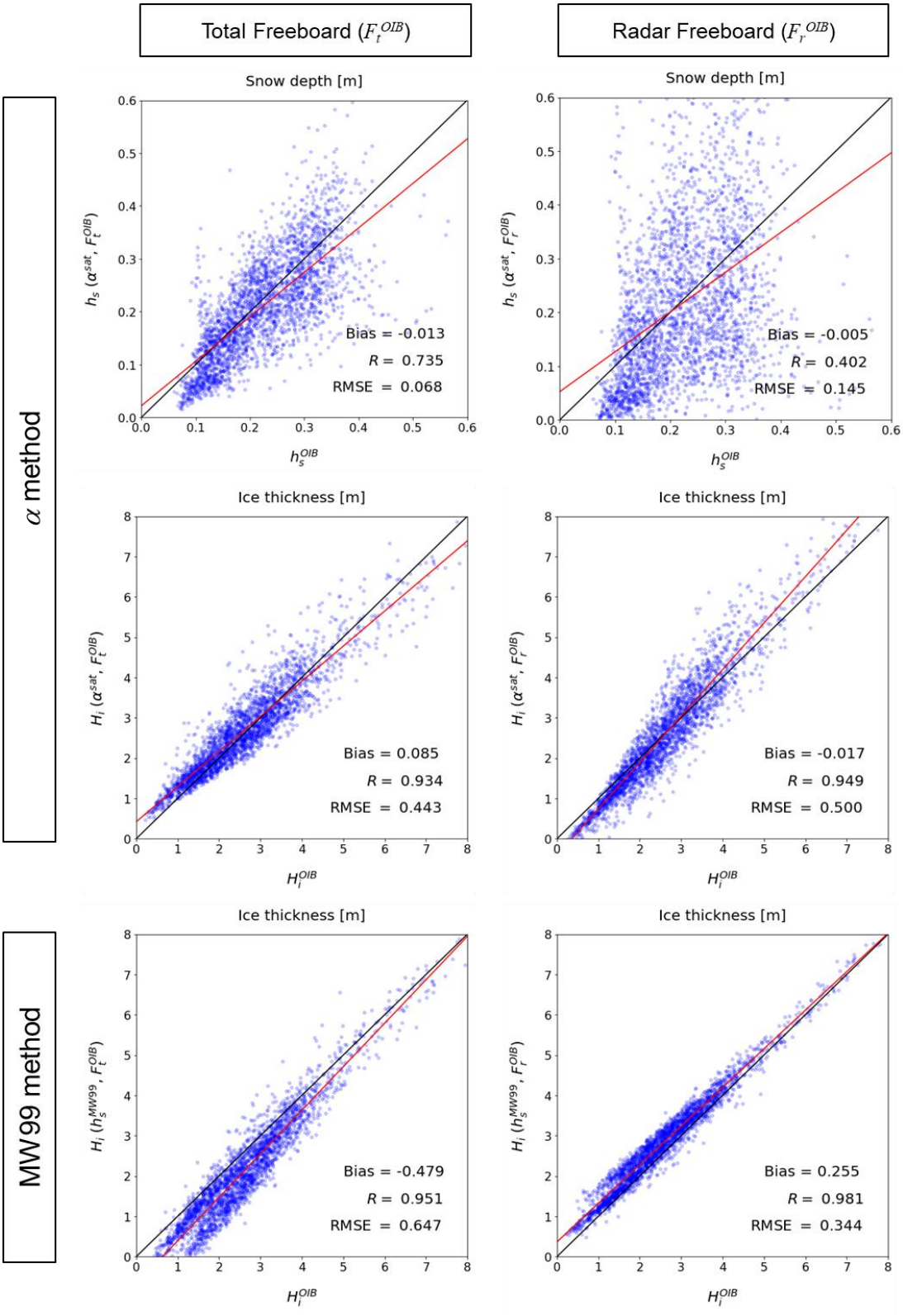

Figure AC1-3. Scatter plots between OIB products and the simultaneously retrieved snow depth and ice thickness from OIB total/radar freeboards during the March 2011–2015 period. Corresponding ice thicknesses estimated from MW99 snow depth are in the third row. The red lines are linear regression lines.

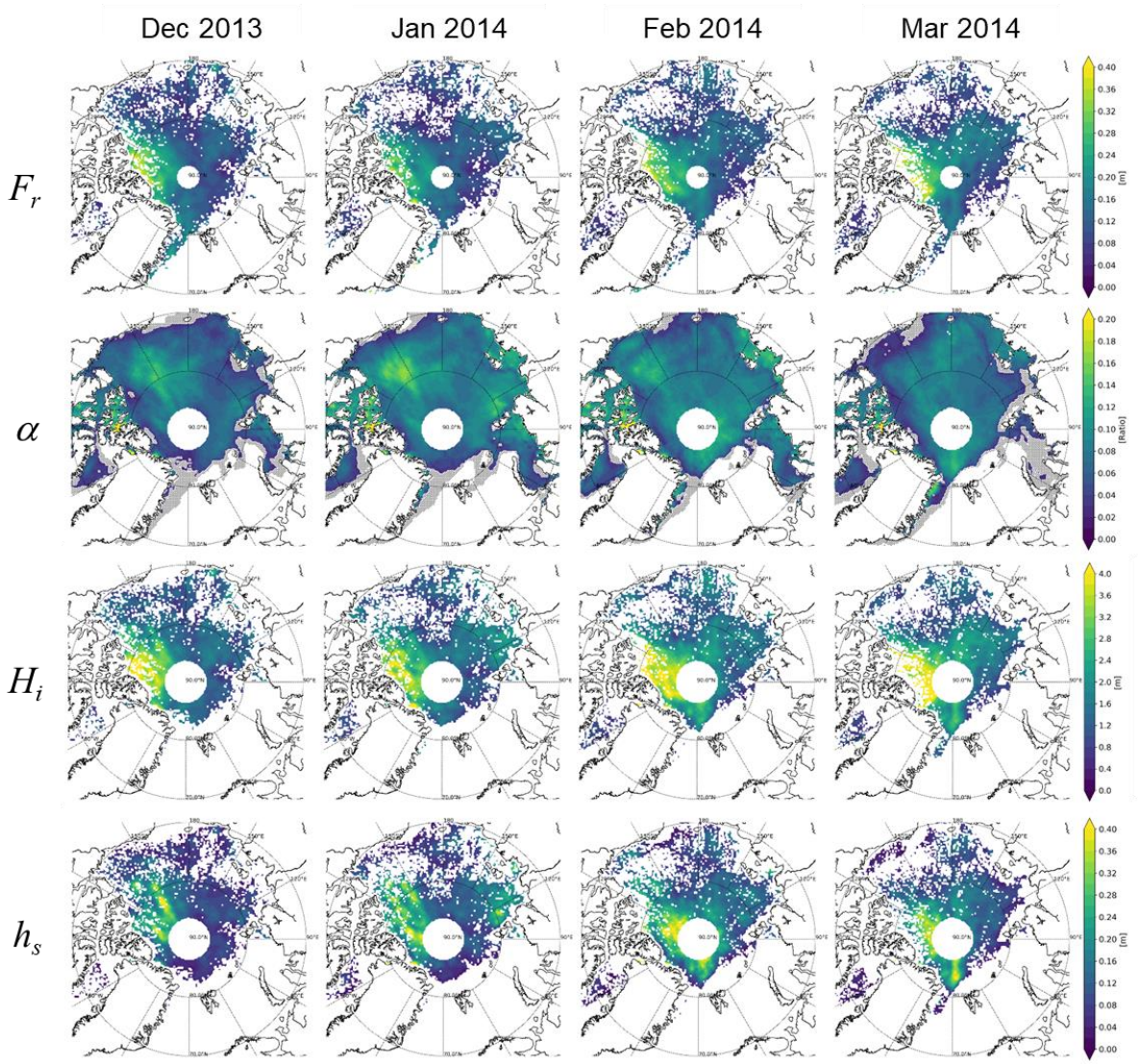

Figure AC1-4. Geographical distributions of observed CS2 radar freeboard (F_r) and estimated snow–ice thickness ratio (α), ice thickness (H_i), and snow depth (h_s) from December 2013 to March 2014. Grey area in the second row denote where α retrieval is failed because T_{as} is warmer than T_{as}.

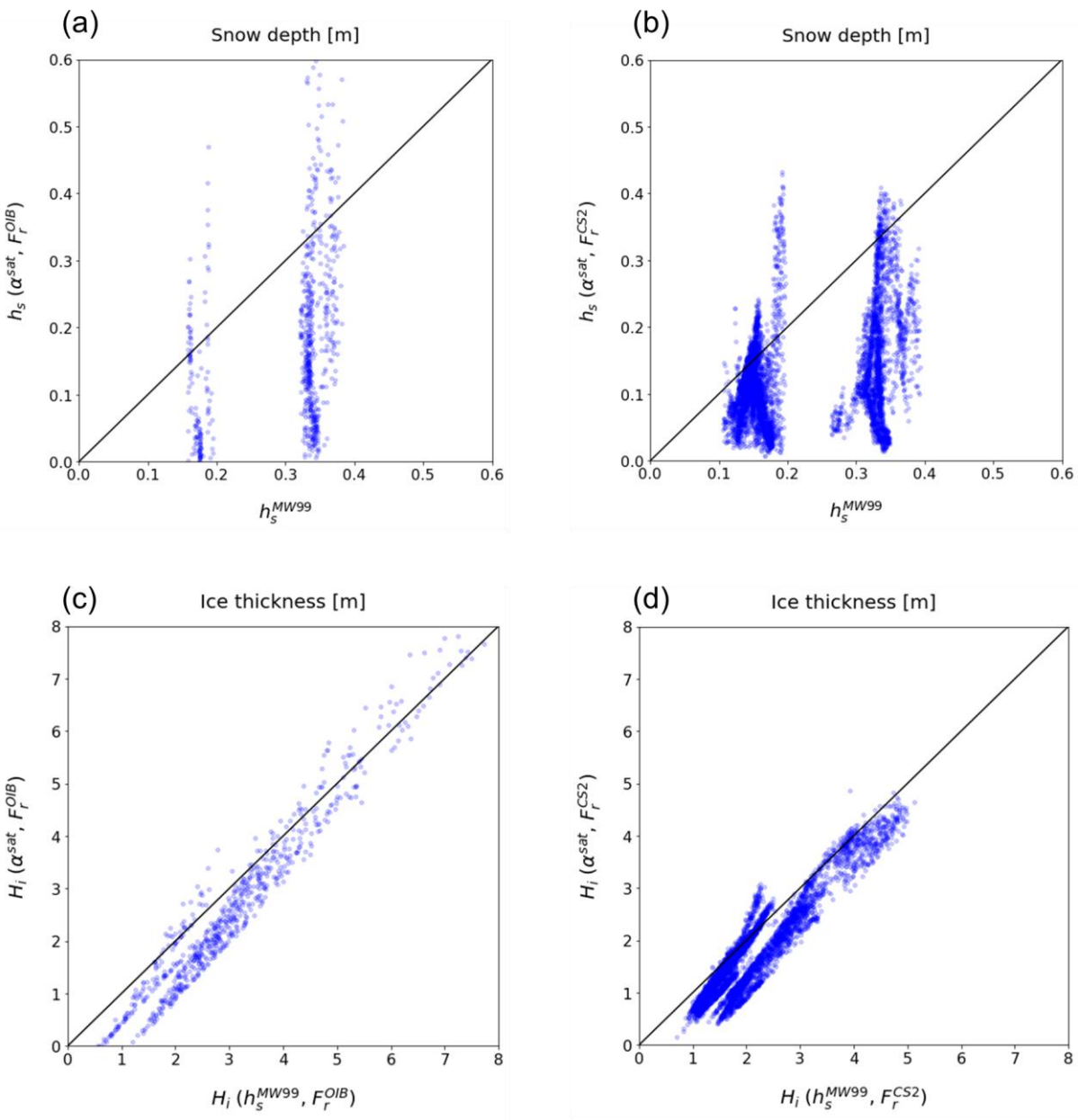

Figure AC1-5. Comparison of simultaneous retrieved snow depth and ice thickness to those from MW99 method. (a) Snow depth from OIB radar freeboard, (b) snow depth from CS2 radar freeboard, (c) ice thickness from OIB radar freeboard, and (d) ice thickness from CS2 radar freeboard.

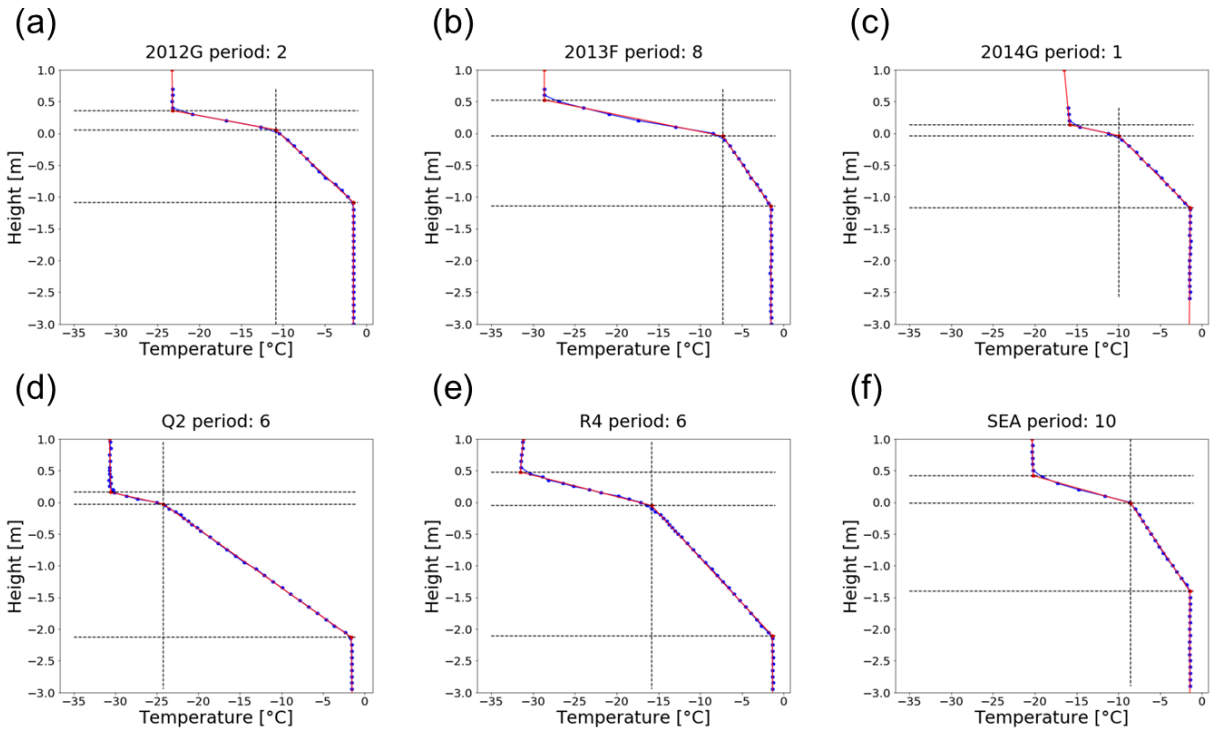

Figure AC1-6. Examples of interface searching results with an averaging period of 15 days: (a) 2012G period 2, (b) 2013F period 8, (c) 2014G period 1, (d) Q2 period 6, (e) R4 period 6, and (f) SEA period 10. The period number is equivalent to the number of time averaging bin. Blue dots are buoy-measured temperature profiles and red lines are regression lines. Black dashed lines indicate the intersections between adjacent regression lines.

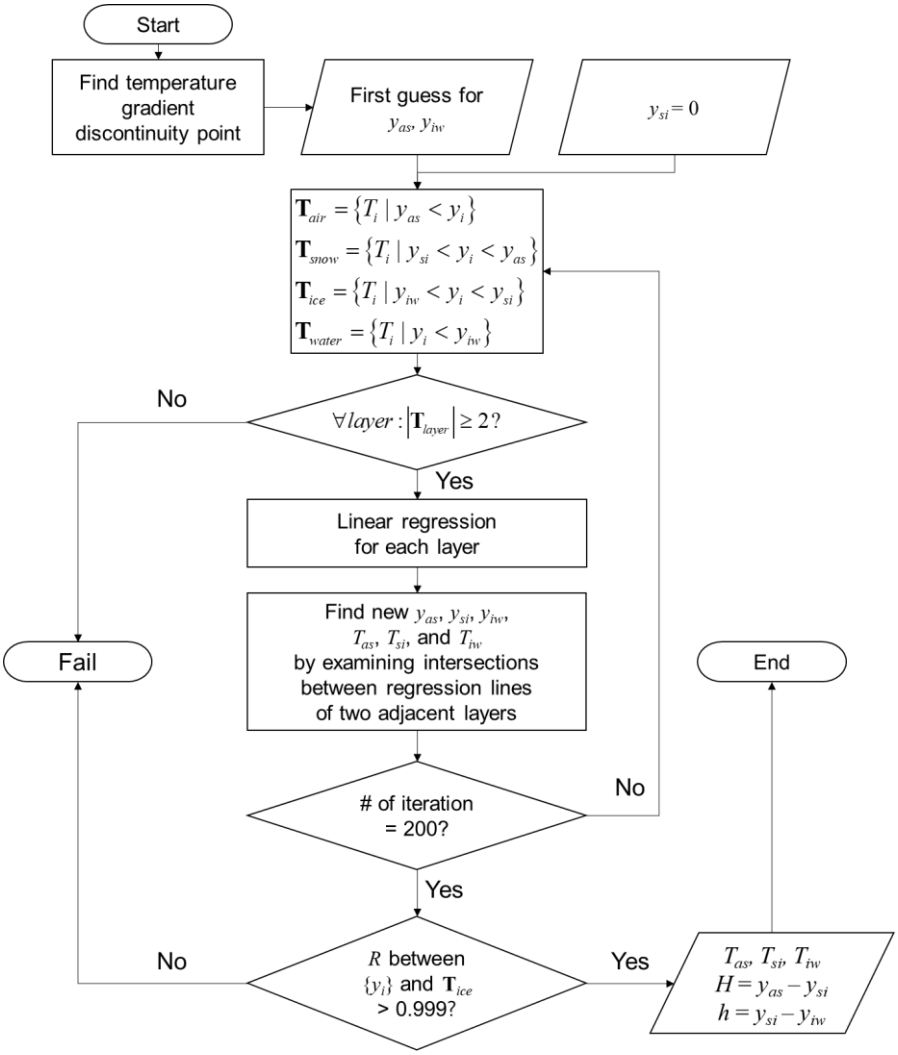

Figure AC1-7. The flow chart of an interface searching algorithm. y_i and T_i denote the position and temperature of a data point in the temperature profile. y_{as}, y_{si}, and y_{iw} denote the position of the interfaces, and $\mathbf{T}_{layer}$ denotes a set of temperature data points.

Appendix B. Sensitivity test for the proposed method

Here we present results of the sensitivity test of showing how the snow depth and ice thickness retrieval results are dependent on the uncertainties in α. To do so, the uncertainty in the snow depth (Δh_s) due to the α error (i.e. $\Delta\alpha$) and associated ice thickness error (ΔH_i) are estimated. From this sensitivity test, we expect to understand why the simultaneous method for the radar freeboard shows more scattered features than those from the method for the lidar total freeboard.

First, Δh_s is defined by the difference of retrieved h_s between with error ($\alpha+\Delta\alpha$) and without error (α).

$$\Delta h_s = \begin{cases} h_s(\alpha+\Delta\alpha, F_t) - h_s(\alpha, F_t) & (\text{using } F_t) \\ h_s(\alpha+\Delta\alpha, F_r) - h_s(\alpha, F_r) & (\text{using } F_r) \end{cases} \quad \text{(B1)}$$

Then, Δh_s can be converted to the error in the ice thickness (ΔH_i) using the following equation derived from Eq. (AC1-5).

$$\Delta H_i = \frac{(f\eta_s - 1)\rho_w + \rho_s}{\rho_w - \rho_i}\Delta h_s = \begin{cases} -6.46\Delta h_s & (\text{using } F_t) \\ 3.44\Delta h_s & (\text{using } F_r) \end{cases} \quad \text{(B2)}$$

Because h_s is a combination of freeboard and α, as in Eq. (AC1-6), we only examine the uncertainty with some representative sea ice types. Here physical states for thicker ice (type A), moderate ice (type B) and thinner ice (type C) are chosen, which are summarized in Table B1. Those typical values are for three types are shown over the scatterplots of OIB-based (α vs. F_t) and of satellite-based (α vs. F_r) – Fig. B1. It is shown that the majority of data points are located around type B, followed by type A. There seem a very small portion of total samples showing values around the type C.

With $\Delta\alpha = \pm 0.03$, which is an RMSE range of the α-prediction equation, Δh_s and ΔH_i are estimated for the three ice types. Results summarized in Table B2 show that $|\Delta h_s|$ is within 5 cm and it tends to decrease as the ice becomes thinner, when the current method is applied to the total freeboard. On the other hand, $|\Delta h_s|$ shows more sensitive behavior for the same $\Delta\alpha$ when the radar freeboard is used for the retrieval. Especially, the sensitivity of type C is the greatest. This is because the denominator of Eq (AC1-6) becomes smaller when α approaches to α_{crit}, resulting in unstable solution. For the ice thickness, $|\Delta H_i|$ is smaller when the total freeboard is used since ΔH_i is proportional to Δh_s. However, the gap between the results from two freeboards has narrowed because H_i from the total freeboard is more sensitive than the radar freeboard to Δh_s, according to Eq. (B2). Sensitivity characteristics shown here are consistent with analysis results given in Sect 4.2. Because there is a much small number of data points belonging to the type C, at least in the data used for this study, the overall sensitivity would likely be in between the B and A types.

It is also of importance to ask to what degree of retrievals is successfully yielded. In this study, cases showing $T_{as} > T_{si}$ or retrieved $\alpha \geq \alpha_{crit}$ are considered to be failures. Statistics on success/fail ratio of α retrieval for December–March of 2011–2015 period are provided in Table B3. Overall, the success ratio was over 82% in December–February, while it was reduced to ~74% in March. Most of failures appear due to the temperature inversion (i.e. $T_{as} > T_{si}$). Regions showing such a temperature inversion are shown with grey shades in the α-distributions of Fig. AC1-4. The grey areas are generally found around the marginal ice zones and in the east of Greenland.

On the other hand, there were near zero failure (0.02% of total pixels) for retrieved $\alpha \geq \alpha_{crit}$. This near zero failure implies that almost all calculated α meet the satisfactory condition after the removal of

cases showing temperature inversion. It may be concluded that calculated α appears to be physically reasonable (i.e. $\alpha < \alpha_{crit}$) as long as presumed thermodynamic conditions are met.

Table B1. Physical state of representative cases of point A, B and C.

Type	H_i **[m]**	h_s **[m]**	α	F_t **[m]**	F_r **[m]**
A	3.961	0.332	0.084	0.65	0.30
B	1.646	0.123	0.075	0.26	0.13
C	0.616	0.152	0.246	0.17	0.01

Table B2. Error of snow depth (Δh_s) and ice thickness (ΔH_i) for snow depth to ice thickness ratio error ($\Delta\alpha$) of ±0.03.

	Total freeboard method		Radar freeboard method	
$\Delta\alpha$	-0.03	0.03	-0.03	0.03
	Δh_s (cm)			
A	-4.070	3.161	-14.59	19.54
B	-1.913	1.471	-5.840	7.730
C	-0.045	0.039	-7.230	37.62
	ΔH_i (m)			
A	0.263	-0.204	-0.502	0.672
B	0.124	-0.095	-0.201	0.266
C	0.003	-0.003	-0.249	1.294

Table B3. Statistics of success/fail ratio α retrieval for 2011-2015 winter.

Year Month	Total Pixels (SIC > 95%)	Success		Fail ($T_{as} > T_{si}$)		Fail ($\alpha > \alpha_{crit}$)	
2010 12	13879	12080	(87.04%)	1799	(12.96%)	0	(0.00%)
2011 01	16246	14004	(86.20%)	2242	(13.80%)	0	(0.00%)
2011 02	17986	14779	(82.17%)	3206	(17.82%)	1	(0.01%)
2011 03	17610	12871	(73.09%)	4738	(26.91%)	1	(0.01%)
2011 12	13915	11405	(81.96%)	2510	(18.04%)	0	(0.00%)
2012 01	16812	13765	(81.88%)	3047	(18.12%)	0	(0.00%)
2012 02	17528	14131	(80.62%)	3397	(19.38%)	0	(0.00%)
2012 03	18741	13586	(72.49%)	5155	(27.51%)	0	(0.00%)
2012 12	14059	11144	(79.27%)	2915	(20.73%)	0	(0.00%)
2013 01	16413	13510	(82.31%)	2903	(17.69%)	0	(0.00%)
2013 02	18640	15526	(83.29%)	3114	(16.71%)	0	(0.00%)
2013 03	19078	14134	(74.09%)	4944	(25.91%)	0	(0.00%)
2013 12	14515	12071	(83.16%)	2444	(16.84%)	0	(0.00%)
2014 01	16880	14201	(84.13%)	2678	(15.86%)	1	(0.01%)
2014 02	16987	14731	(86.72%)	2247	(13.23%)	9	(0.05%)
2014 03	17699	13300	(75.15%)	4391	(24.81%)	8	(0.05%)
2014 12	14071	11119	(79.02%)	2952	(20.98%)	0	(0.00%)
2015 01	17008	15095	(88.75%)	1913	(11.25%)	0	(0.00%)
2015 02	18076	15907	(88.00%)	2169	(12.00%)	0	(0.00%)
2015 03	17618	14042	(79.70%)	3576	(20.30%)	0	(0.00%)
December	70439	57819	(82.08%)	12620	(17.92%)	0	(0.00%)
January	83359	70575	(84.66%)	12783	(15.33%)	1	(0.00%)
February	89217	75074	(84.15%)	14133	(15.84%)	10	(0.01%)
March	90746	67933	(74.86%)	22804	(25.13%)	9	(0.01%)

α_{crit}=0.291 for ρ_s=320 kg m^{-3}, ρ_i=915 kg m^{-3}, ρ_w=1024 kg m^{-3}, and f=0.84.

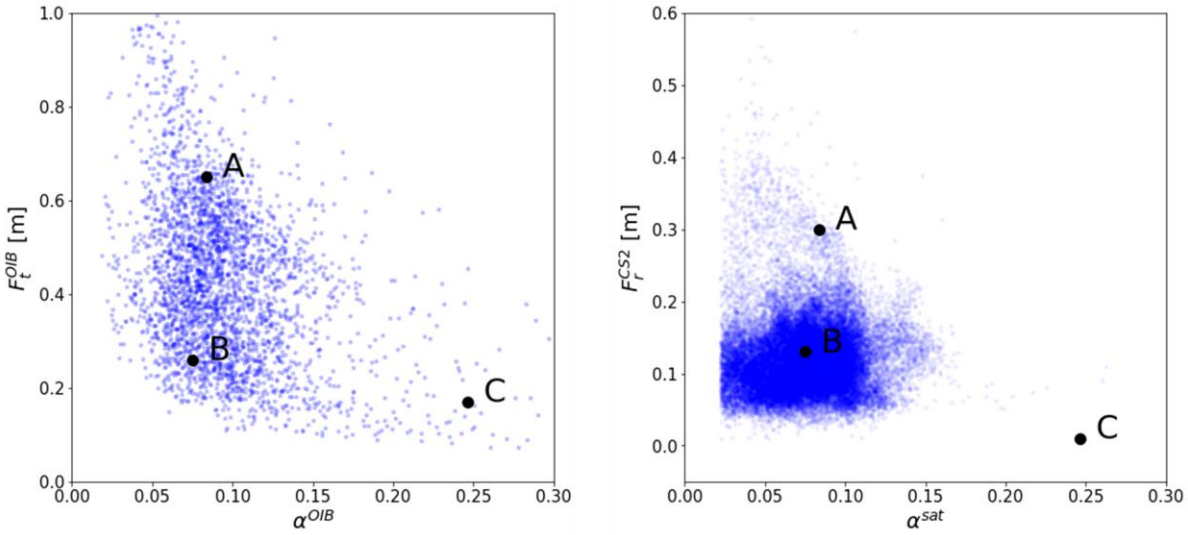

Figure B1. Location of physical state of representative types (A, B, C) on the freeboard-thickness ratio space. Blue dots are from (left) OIB data and (right) retrieved thickness ratio and CS2 radar freeboard.